MULTISOURCE DATA INTEGRATION: COMPARISON OF GEOMETRIC AND RADIOMETRIC METHODS♥

Thierry Toutin
Canada Centre for Remote Sensing
588 Booth Street, 3rd Floor
Ottawa, Ontario, Canada, K1A 0Y7

Abstract

Multisource data integration requires geometric and radiometric processing adapted to the nature and characteristics of the data in order to keep the best information from each image in the composite image. This article compares different geometric and radiometric processing techniques and evaluates, quantitatively and qualitatively, their impact on the resulting composite images, using panchromatic SPOT and airborne SAR images. The techniques that take into account the nature of the data give better results, with greater integrity: subpixel geometric accuracy and high-quality composite images which are sharp and precise, containing well-defined cartographic elements and data that are easy to interpret and closer to physical reality.

1. Introduction

The processing of multisource data can be based on the concept of "geocoded images", a term originally invented in Canada in defining value-added products (Guertin and Shaw, 1981). Photogrammetrists, however, prefer the term "ortho-image" in referring to a unit of geocoded data. To integrate different data under this concept, each raw image must be separately converted to an ortho-image so that each component ortho-image of the data set is registered pixel by pixel and the different radiometries can then be combined (Clark, 1980).

There are many references in the literature which combine and/or compare the data in the visible and microwave spectra. The early work by Murphrey (1978), Anuta et al (1978), Daily et al (1979), Guindon et al (1980) and many others dealt mainly with the integration of Landsat and Seasat data, although other geocoded data were also used (Zobrist et al, 1979).

The method most commonly used is image-by-image registration to a previously geocoded reference image. This registration uses polynomial or spline functions with many tie points between the images. However, the authors generally report the difficulty of finding such tie points between the images, because they are imaged differently by sensors which have highly variable geometries and responses to

---

♥ Translations from French: Intégration de données multi-sources : comparaison de méthodes géométriques et radiométriques, International Journal of Remote Sensing, 1995, Vol. 16, No. 15, pp. 2795-2811.

illumination. The errors resulting from this method are of a few pixels, which then generate errors in the radiometric merging of the various ortho-images. The effect is even more significant in mountainous terrain.

To find tie points between an airborne radar image (pixel of 4 $\times$ 4.31 m) and a Landsat-TM image, Guindon (1985) used the automatic correlation of quicklooks. The correspondence errors of ±20 m will also generate poor merging of radiometric information; moreover, without knowledge of the type of image, illumination angles and other viewing conditions, it is difficult to generalize this result to other types of images, especially since the advent of new sensors such as those of SPOT, ERS-1 and JERS-1, and others.

The purpose of this article is to demonstrate the attraction of geometric and radiometric processing techniques suited to the nature and characteristics of the different data, and to measure the impact of the processing methods on the integration and quality of the resulting image, by:

- comparing different geometric and radiometric methods of integrating multisource data;
- evaluating, quantitatively and qualitatively, the impact of these different methods on the resulting composite image.

Two types of very different images were selected to make the experiment more difficult and to take into account the complementary aspects of visible versus microwave and airborne versus satellite: a panchromatic SPOT image (SPOT-P) and airborne synthetic-aperture radar (SAR) images.

Two methods of geometric correction were compared: the polynomial functions generally used and a rigorous photogrammetric method developed at the Canada Centre for Remote Sensing (CCRS) and tested on different images. For the latter method, the same SRIT software ("Système de Rectification des Images de Télédétection") (Toutin and Carbonneau, 1992) was used for both image types. In addition, this method allows the integration of a digital elevation model (DEM) into the correction.

Four methods of merging the spectral information from the SPOT-P and airborne SAR ortho-images were evaluated: red-green-blue, principal components, intensity-hue-saturation and high-pass filter.

2. Description of the data

The cartographic data are those of the Sherbrooke test area (Quebec, Canada) for topographic applications of remote sensing (Lasserre and Lemieux, 1990). The test area comprises two 1:50,000 map sheets: the north half of sheet 21E4 (Coaticook) and the south half of sheet 21E5 (Sherbrooke) (Figure 1); this covers a land area of about 26 km by 40 km. The maximum elevation difference in this area is 350 m, with slopes of up to thirty degrees in the alpine ski resorts. The data used in this research consist of:

- paper maps at scales of 1:50,000 and 1:250,000;

- the digital file of position data for the cartographic elements, as observed on the Earth's surface in X, Y and Z coordinates, without shifting of the elements through cartographic generalization; these were acquired by stereodigitization (B8-S, 2nd order), with a root-mean-square accuracy of about three metres; these data are unstructured (without topology) and are not cleaned (error of closure and of segmentation at the intersections);
- a hundred or so ground points, including map coordinates, acquired using a STK-1 stereo comparator with a root-mean-square accuracy of one to three metres; these points are mainly intersections of expressways, highways, roads and railways; and
- a DEM with an interval of 50 m, derived from the elevation contour lines (10 metres apart) from the 1:50,000 map; the root-mean-square accuracy is about five metres.

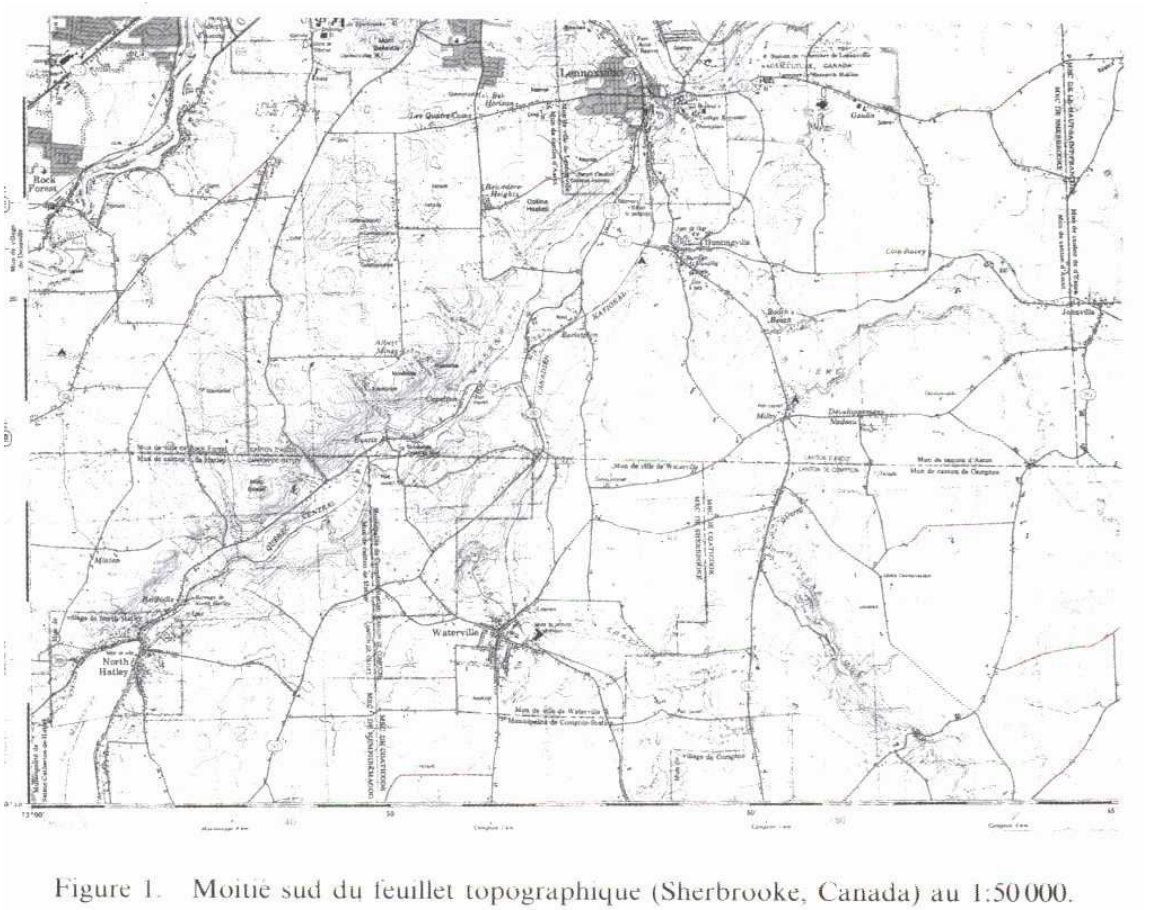

Figure 1. Moitié sud du feuillet topographique (Sherbrooke, Canada) au 1:50 000.

Figure 1: South half of topographic map sheet (Sherbrooke) at 1:50 000

The remote sensing data consist of:

- a SPOT-P raw image (level 1) acquired June 20, 1987 at a highly tilted viewing angle (+29.3°) and the ephemeris and attitude data related to this image;
- four airborne SAR images (north-south direction) acquired September 11, 1990 by the IRIS sensor of CCRS (C-HH, narrow mode, angle of 45° to 76°, ground distance, 4096 pixels by 10,000 lines, pixel spacing 4.0 $\times$ 4.31 m) (Livingstone et al, 1987).

Since the width of a SAR image swath is approximately 16 km, two images were taken pointing east and two pointing west to create two radiometrically different SAR mosaics over the test area (26 $\times$ 40 km).

The SPOT-P image has a grey-scale dynamic range of 17 to 60. No radiometric processing was done, except linear stretching on 8 bits.

The SAR images were processed in real time in the aircraft and were encoded on 8 bits. No radiometric processing was done of these images.

3. Description of the processing techniques

The composite images are products resulting from the integration of multisource data. Their creation requires two distinct processing operations to ensure that those elements, which are spatially and spectrally separable in the original images are also separable in the composite images:

- geometric processing to ensure that each pixel in the ortho-images corresponds to the same ground element;
- radiometric processing to merge the information from each image in a common image, such that this common image preserves the best spectral information from each image.

3.1 Geometric processing

While it is known that polynomial functions are not suitable for accurately correcting airborne or space images, many users still apply them, without knowing the implications for subsequent processing operations and the resulting products. The purpose of this comparison is primarily to evaluate and show the impact of these various processing techniques on the results and the composite image.

For both methods (polynomial and photogrammetric), the processing steps are more or less similar, except for the viewing parameters and the altimetry (ground control points and DEM) involved in the photogrammetric method:

- acquisition of the parameters of the viewing geometry (for the photogrammetric method only);
- acquisition of the ground control points: image coordinates and ground coordinates X, Y, (Z);
- calculation of the parameters of the polynomial or photogrammetric model;
- cubic-convolution resampling (with DEM) to create the ortho-images and mosaics, with the same pixel size (5 m);
- registration of the vector file to check the results.

Since the polynomial methods, with their formulation, are well known and documented in Colwell (1983), only a few characteristics are given. The polynomial function of the 1st degree allows to correct a translation, a rotation, a scaling in both axes and an obliquity. Polynomial functions of a higher degree (mainly 2nd and 3rd) enable us to

correct larger distortions. However, they are generally limited (small image, flat ground and so on), as they do not reflect the causes of distortions during formation of the image. Moreover, one of the assumptions of these functions is that the ground is flat (with no curvature of the Earth), and without relief.

The photogrammetric model, with its formulation, has been described in detail for SPOT-HRV images (Toutin, 1986) and for other types of images (Toutin et al, 1992). This model represents the physical law of transformation of ground space to image space. The development of the final equations is based on principles related to photogrammetry (collinearity condition), orbitography (flight path represented by an osculatory ellipse), geodesy (use of a reference ellipsoid) and cartography (conformity of the projection).

The application of these principles in the development of the final equations was detailed in Toutin, 1986; they allow integration and combination with each other of the different distortions during formation of the image, as follows:

- distortions related to the platform (position, velocity, orientation);
- distortions related to the sensor (orientation angles, line integration time, instantaneous field of view);
- distortions related to the Earth (geoid-ellipsoid), including relief; and
- distortions related to the map projection (ellipsoid-map plane).

The main characteristics and comparison of the two methods (polynomial and photogrammetric) are summarized in Table 1 (Colwell, 1983; Toutin and Carbonneau, 1989).

Table 1: Comparison of characteristics for both methods

POLYNOMIAL METHOD	PHOTOGRAMMETRIC METHOD
Does not respect the viewing geometry	Respects the viewing geometry
Not related to distortions	Reflects the distortions
Does not introduce attitude data	Uses ephemeres and attitude data
Does not use DEM	Uses DEM or near elevation
Corrects image locally at the GCPs	Corrects the image globally
Does not filter blunders	Filters blunders with the knowledge of the geometry
Individual adjustments of one image	Simultaneous adjustment of more than one image
Image-to-image correction	Image-to-ground correction
Needs many (>20) GCPs	Need few (3-8) GCPs
Sensitive to GCPs distribution	Not sensitive to GCPs distribution
Problem of choice for tie points	GCPs choice as a function of each image

3.2 Radiometric processing

There are a number of methods for merging spectral information from different images (Chavez et al, 1991):

- red-green-blue coding (RGB);
- principal component analysis (PC);
- intensity-hue-saturation coding (IHS); and
- high-pass filter (HPF).

RGB coding is used directly with three images, assigning each ortho-image to a colour: SPOT-P in red, SAR-west in green and SAR-east in blue.

The PC method is a statistical method, which by linear combination transforms a data set of variables correlated among themselves into new decorrelated variables. This method generates new orthogonal axes in radiometric space called principal components. The sum of the variance remains unchanged and each consecutive PC has a decreasing level of variance. Depending on the case in question, the first three PCs are used or one of the PCs can be replaced by another image. In the case of three images, these are the three PCs used.

IHS coding can be used in two ways:

(1) the images are used directly to modulate the RGB display of the IHS coding; some authors use the image with the higher spatial resolution, or the SAR, for intensity (Jaskolla et al, 1988), while others advise modulating saturation rather than intensity (Welch and Ehlers, 1988);

(2) the IHS parameters are calculated on the basis of three images or spectral bands, then one of the parameters is replaced by a fourth image (of higher resolution, or a SAR) and the RGB reverse transformation is performed to merge the images.

Since we only had three ortho-images, only the first method of IHS coding was used in the comparisons of the various radiometric merges.

In the HPF method, we use a high-pass filter to process the image with the highest spatial resolution and then combine it, pixel by pixel, with the image having the lowest spatial resolution but the highest spectral resolution. Thus this method combines the spatial information from the image of higher spatial resolution with the spectral information from the image of higher spectral resolution. It applies mainly to combining a SPOT-P or SAR image with a Landsat-TM or SPOT-XS multiband image; this is not the case we are considering with one SPOT-P image and two SAR images.

4. Analysis of the results

4.1 Geometric processing

Analysis of the geometric processing results is done in two stages:

- quantitative analysis involving the residuals on the ground control points (GCPs), the errors on the independent check points (ICPs) and comparison with the vector file;
- qualitative analysis involving a comparison of the cartographic elements (roads, rivers, forest, cutovers and so on) on the two ortho-images.

Table 2, based on 15 ground control points (GCPs), gives the root-mean-square and maximum residuals (in metres) of the calculation of geometric correction models for the photogrammetric method and the polynomial methods (2nd and 3rd orders). Although in the photogrammetric method only four ground control points for SPOT-P and seven for SAR are necessary and the photogrammetric model is not sensitive to the number of GCPs (Toutin and Carbonneau, 1989), 15 GCPs were used for consistency in the comparison of results.

Table 2: Root mean square and maximum residuals (metres) on 15 GCPs

IMAGE / **METHOD**	**RES.**	**SPOT-P**		**SAR1-WEST**		**SAR2-WEST**		**SAR1-EAST**		**SAR2-EAST**		**ALL**	
Residuals		Rx	Ry	Rx	Ry	Rx	Ry	Rx	Ry	Rx	Ry	Rx	Ry
Photogram-metric	RMSR	2,7	3,1	1,0	2,5	6,3	4,9	6,1	6,1	2,9	4,3	3,5	3,6
	Rmax	- 5,0	7,6	- 1,7	4,4	-10,2	-9,9	10,0	10,6	6,4	10,6	7,8	-7,3
Polynomial 2nd order	RMSR	23,1	3,4	4,9	3,7	13,8	4,4	14,0	6,3	13,2	5,1	-	-
	Rmax	-50,3	6,0	-10,8	7,4	-20,8	11,6	-29,6	-9,3	-26,3	-9,7	-	-
Polynomial 3rd order	RMSR	18,7	1,3	4,6	2,6	9,5	3,6	10,1	6,1	9,9	4,5	-	-
	Rmax	-40,6	- 2,4	- 9,4	6,2	-20,2	7,4	-27,3	-7,8	-23,1	-8,5	-	-

The residuals are better for the photogrammetric method than for the polynomial methods. In the X direction, the deviation is more visible because of the elevation distortions, which are modelled in the photogrammetric method.

In addition, this method allows simultaneous adjustment of all images by using points common to two or more images as tie points (coplanarity condition). This simultaneous adjustment provides better relative accuracy between the images.

In the photogrammetric method, the residuals are a good indicator of the final accuracy (Toutin and Carbonneau, 1989), since the correction model is one that corrects the image globally. The same is not true of the polynomial methods, which correct locally at the ground control points, but distortions between the GCPs are not entirely eliminated because they are not rigorously modelled.

The fact that the residuals of the 3rd-order polynomial method are better than those of the 2nd order does not imply better accuracy. In the 3rd order, in fact, as there are eight

additional unknowns and the same number of GCPs, the degree of freedom in the least squares adjustment is smaller, and thus reduces the adjustment residuals.

Since we know the value of the 3rd-order unknowns calculated for each image, we can determine their effect on the ground or their contribution in the correction:

- for SPOT-P, we have: $3.7\ 10^{-13} \times 6{,}000^3 < 0.1$ m;
- for SAR, we have: $2.5\ 10^{-12} \times 4{,}096^2 \times 10{,}000 < 0.5$ m;
  $4.5\ 10^{-15} \times 10{,}000^3 < 0.01$ m.

These 3rd-order parameters are negligible and have no effect in the correction. Despite the results of the residuals, the 3rd-order polynomial does not allow better correction of the images.

Moreover, calculated on twenty or so check points (ICPs) plotted on the ortho-images, the errors are greater (10-20 m) with the 3rd-order polynomial method than with that of the 2nd order. For these reasons, the analysis of the results and the comparison of the ortho-images and their merging will not take the 3rd order into consideration.

Table 3 gives the root-mean-square errors, maximums and bias calculated on about fifty ICPs for the photogrammetric and 2nd-order polynomial methods. These ICPs, plotted on the ortho-images, are different from the 15 GCPs used in calculating the geometric correction models. The errors therefore reflect the final accuracy of the products.

Table 3: Root mean square, maximum and bias errors (metres) on 50 check points

IMAGE / **METHOD**		**SPOT-P**		**SAR1-WEST**		**SAR2-EAST**		**SAR1-EAST**		**SAR2-EAST**	
Errors		Ex	Ey	Ex	Ey	Ex	Ey	Ex	Ey	Ex	Ey
Photogrammetric	RMQE	3,8	3,4	5,0	4,3	10,9	6,6	9,1	9,0	7,5	7,6
	Emax	-8,7	- 9,9	-11,7	8,5	-24,4	-20,2	23,7	-22,8	-17,6	15,1
	Bias	1,4	- 0,1	0,2	0,0	0,3	0,3	4,1	- 1,8	0,3	- 1,2
Polynomial 2nd order	RMQE	30,0	16,3	13,3	10,3	21,8	14,6	15,7	10,0	21,4	9,1
	Emax	-68,1	31,8	-35,7	-25,2	-46,0	35,1	46,9	27,5	-61,8	-17,5
	Bias	-11,8	11,5	- 1,8	-1,4	3,8	- 2,9	3,9	- 0,2	3,4	- 3,3

In any case, the photogrammetric method gives better results than the polynomial method. Note that, for SPOT-P, the differences between the two methods are significantly greater, since modelling of the satellite orbit with the ephemeris is much more accurate than modelling of the aircraft flight with only approximate values for altitude, direction and speed.

As in Table 2, the differences are still greater in the X direction, primarily because of the altimetry effects, which are not corrected in the polynomial method.

The SAR-west and SAR-east mosaics and integration of the three ortho-images will therefore be achieved with an absolute error of:

- 10-15 m in the X and Y directions for the photogrammetric method; and
- 30-40 m in the X and Y directions for the polynomial method.

The qualitative evaluation of these geometric processing techniques is performed on the ortho-images and on the colour composite, which has been generated with the IHS coding. Since the total ortho-image represents 30 $\times$ 40 km with a pixel of five metres, subimages representative of the whole are used for this qualitative evaluation for a better view of the details and differences.

Figure 2 is a comparison of two composite subortho-images (4 $\times$ 3 km; pixel of 5 m) by the photogrammetric method (top) and by the polynomial method (bottom) to which the road vector file (accuracy of 3-5 m) has been registered. The radiometric processing operations performed are the same for both images.

The top image is much more homogeneous in its colours, surfaces and variations. As there is greater contrast between the elements, their boundaries are clear and well defined.

In the bottom image, the colour variations are greater, giving an impression of texture, and the image seems more blurred. As there is less contrast between the elements, they appear less well defined.

Using the vector file from the topographic map, the analysis of certain cartographic elements showed, in the bottom image (letters a, b and so on refer to parts of the image identified in Figure 2), that:

a: the linear elements (roads and rivers) are doubled or even disappear (bridge, roads), which corresponds to a relative error of registration;
b: the lack of sharpness in this part prevents us from distinguishing the road from the forest and areas of bared soil;
c: on surface elements, artifacts are created; there is an inversion between forest (green) and cutovers (burgundy);
d: the texture and colour variations do not correspond to the real information.

These examples, with other similar ones which can be counted on these subimages, clearly show that the geometric registration errors have generated radiometric merging errors, artifacts and erroneous information in the composite image which do not correspond to any physical reality.

The road vector file, registered to these subimages, allows us to check the geometric accuracy: the visual analysis confirms the earlier statistical results for the polynomial method (30-50 m), but shows an improvement for the photogrammetric method (10 m), with maximum errors of 20 metres. Checks on other parts of images show the consistency of the results. These values correspond to the absolute error of registration.

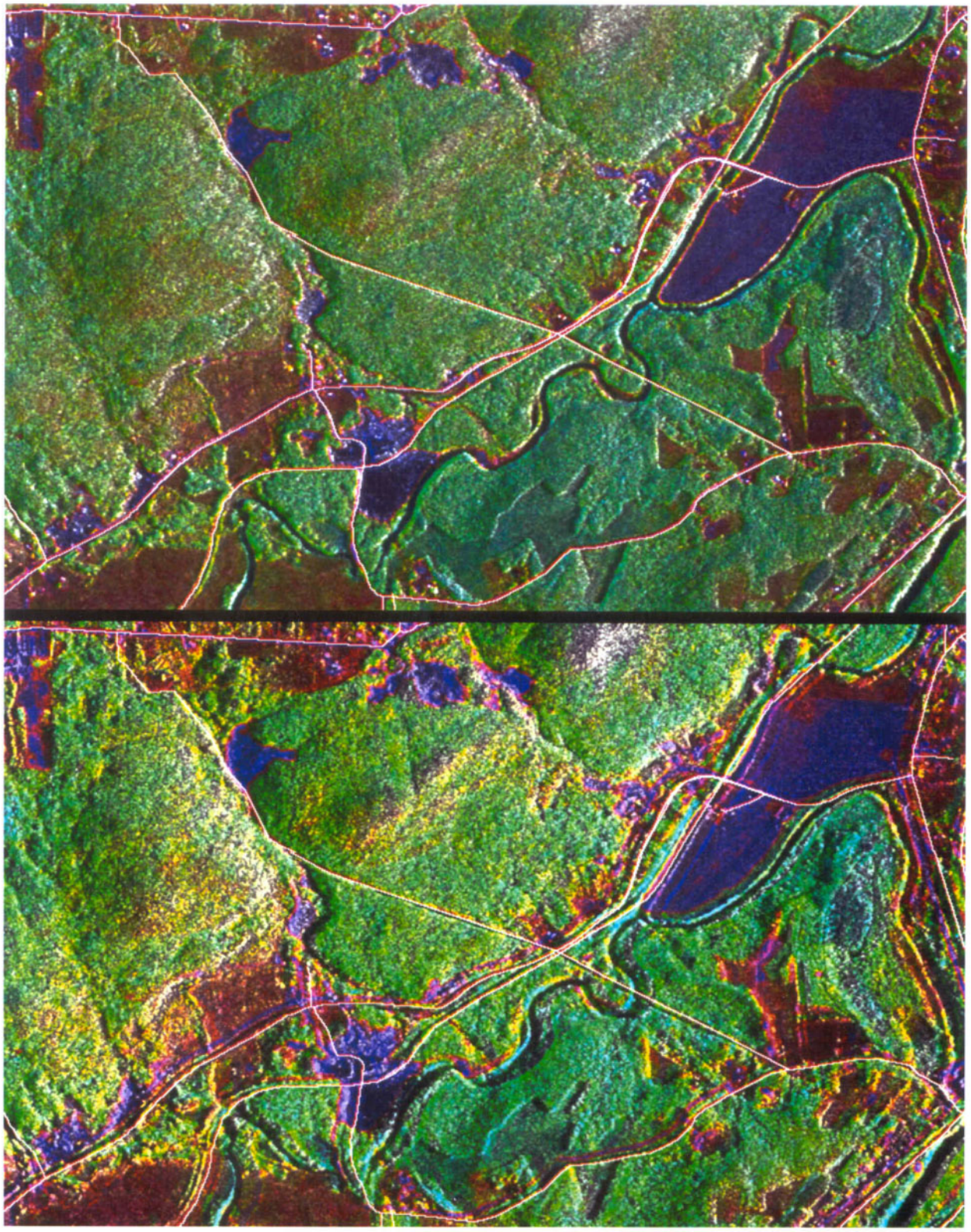

Figure 2: Composite subortho-images (4 x 3 km; 5 m pixel spacing) with overlay of digital road network file: 2D polynomial method (below), and 3D photogrammetric method (above)

4.2 Radiometric processing

As the analysis of geometric processing operations has shown that the polynomial methods affect the geometry and radiometry of the composite image, the radiometric processing operations described in 3.2 are performed only on the ortho-images geocoded by the photogrammetric method. For better detail visibility, only subimages (10 $\times$ 10 km; pixel of 5 m) are given.

RGB coding is used directly by assigning SPOT-P to red, SAR-west to green and SAR-east to blue (Figure 3). In this combination, the characteristics of each image (SPOT-P, SAR) are well preserved. The highly visible elements on SPOT-P come out in red, and the elements oriented west and east come out in green and blue respectively. This is especially visible on river banks.

The PC analysis showed that the three ortho-images were practically decorrelated and that:

- the first PC is 99% formed of SPOT-P;
- the second PC is 97% formed of SAR-west; and
- the third PC is 97% formed of SAR-east.

Thus using the three PCs contributes no more than using the three original ortho-images. Moreover, the results are often more difficult to interpret quantitatively and qualitatively because, as the statistical properties have been manipulated, the original integrity of the data has not been preserved (Harris et al, 1990).

After various combinations for the IHS coding were tested, two which differed from each other were selected:

(1) Figure 4 combines SPOT-P in I, SAR-west in H and SAR-east in S;
(2) Figure 5 combines SAR-west in I, SPOT-P in H and SAR-east in S.

The image in Figure 4 somewhat resembles a colour air photo in which many characteristics of SARs are not visible (texture, relief and so on). Since SPOT-P was assigned to intensity, which represents the brightness of colour, the highly visible elements on SPOT-P come out as very light. As SAR-west was assigned to hue, which represents the dominant colour, it does not help provide much colour variation.

The image in Figure 5 has very good visual quality and effectively combines the characteristics of the various original images. It also shows much more texture because of the SAR-west assigned to intensity. The colour contrast between the forests, fields and bared soil areas is quite pronounced.

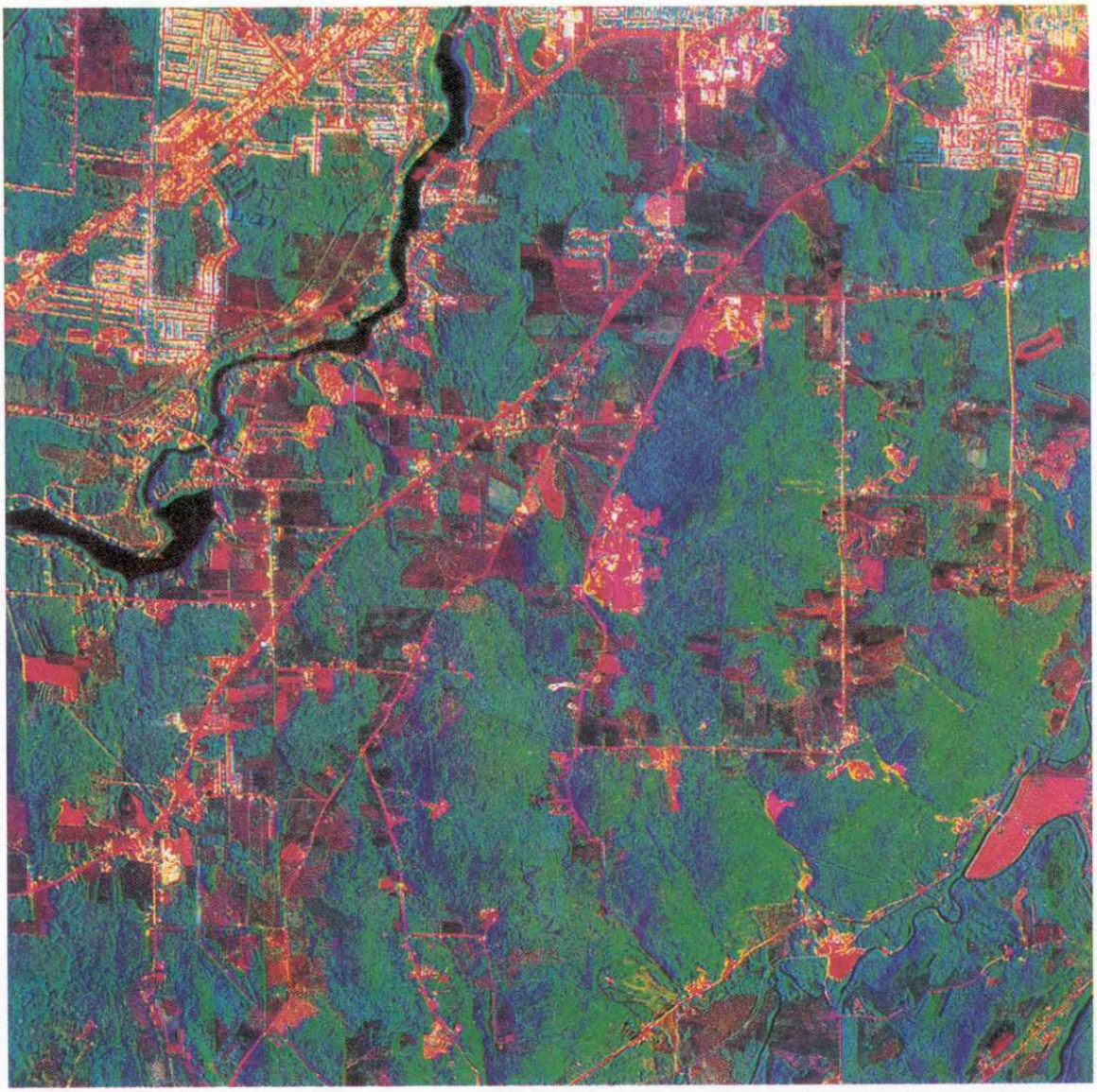

Figure 3. Sous-ortho-image composé (10 km sur 10 km; pixel de 5 m) en utilisant le codage RVB (SPOT-P/RAS-ouest/RAS-est).

Figure 3: Composite sub ortho-images (10 x 10 km; 5 m pixel spacing) using RGB coding (SPOT-P/SAR-west/SAR-east)

To compare the results of these different methods, we can visually interpret the image content of the three composite images for the conventional applications of remote sensing: topographic mapping, agriculture, forestry and geology. While this is not an in-depth, exhaustive interpretation, it enables us to demonstrate the main elements which can be extracted from each composite ortho-image and to determine for each application the best combination or combinations of SPOT-P and two SARs.

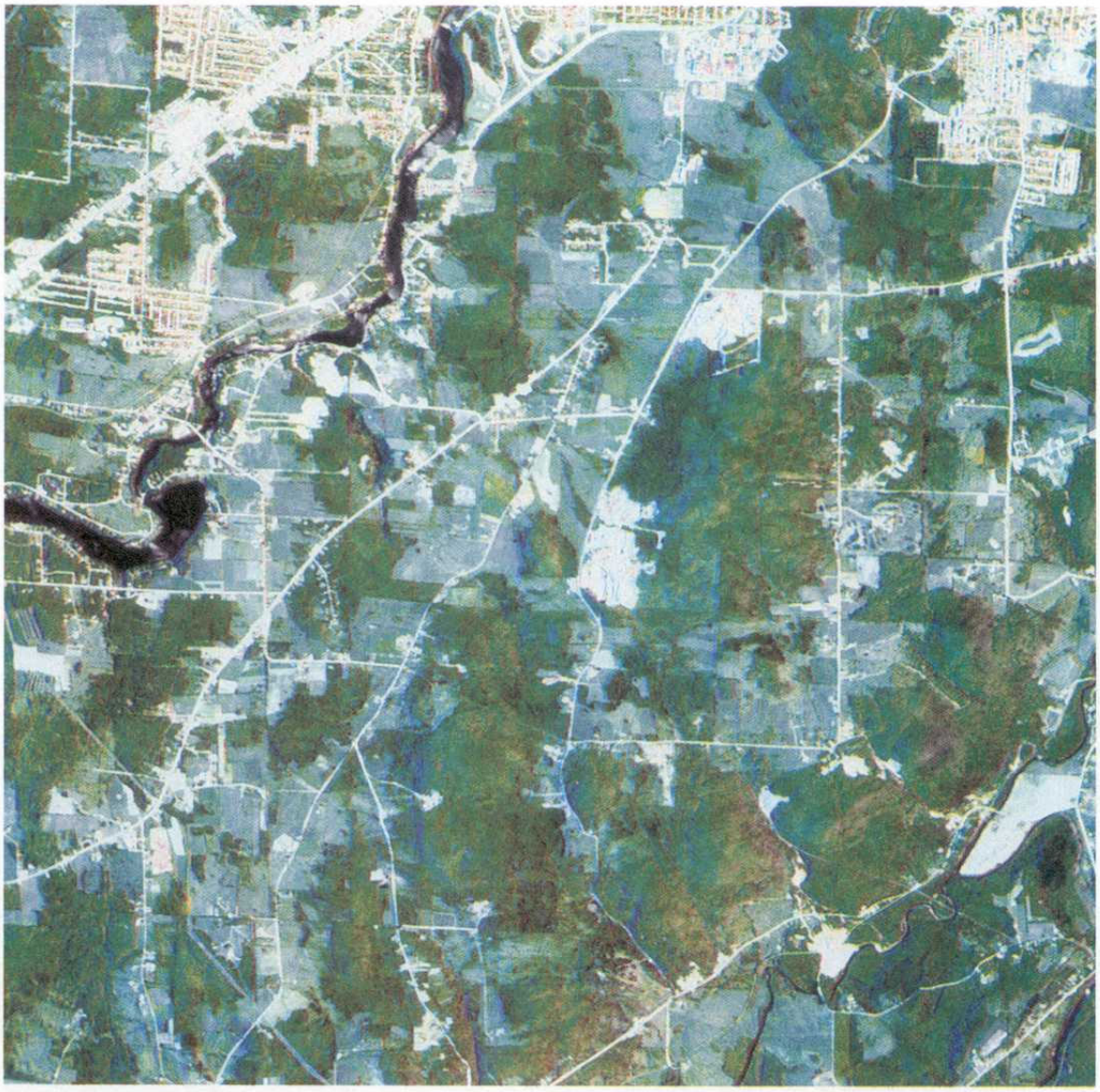

Figure 4. Sous-ortho-image composée (10 km sur 10 km; pixel de 5 m) en utilisant le codage ITS (SPOT-P/RAS-ouest/RAS-est).

Figure 4: Composite subortho-images (10 x 10 km; 5 m pixel spacing) using IHS coding (SPOT-P/SAR-west/SAR-east)

4.2.1 Topographic mapping

In the three images, roads can be distinguished easily because of the spatial resolution (5 m) and the contrast with other elements. In the image in Figure 4, however, they are confused with the buildings and built-up areas because of the lack of colour contrast. Similarly, the roads in new residential developments in forested areas are not visible in this image, while they are clearly visible in the other two. For rivers, there is little colour variation from the SPOT-P and the moderate contrast only allows us to distinguish the boundaries.

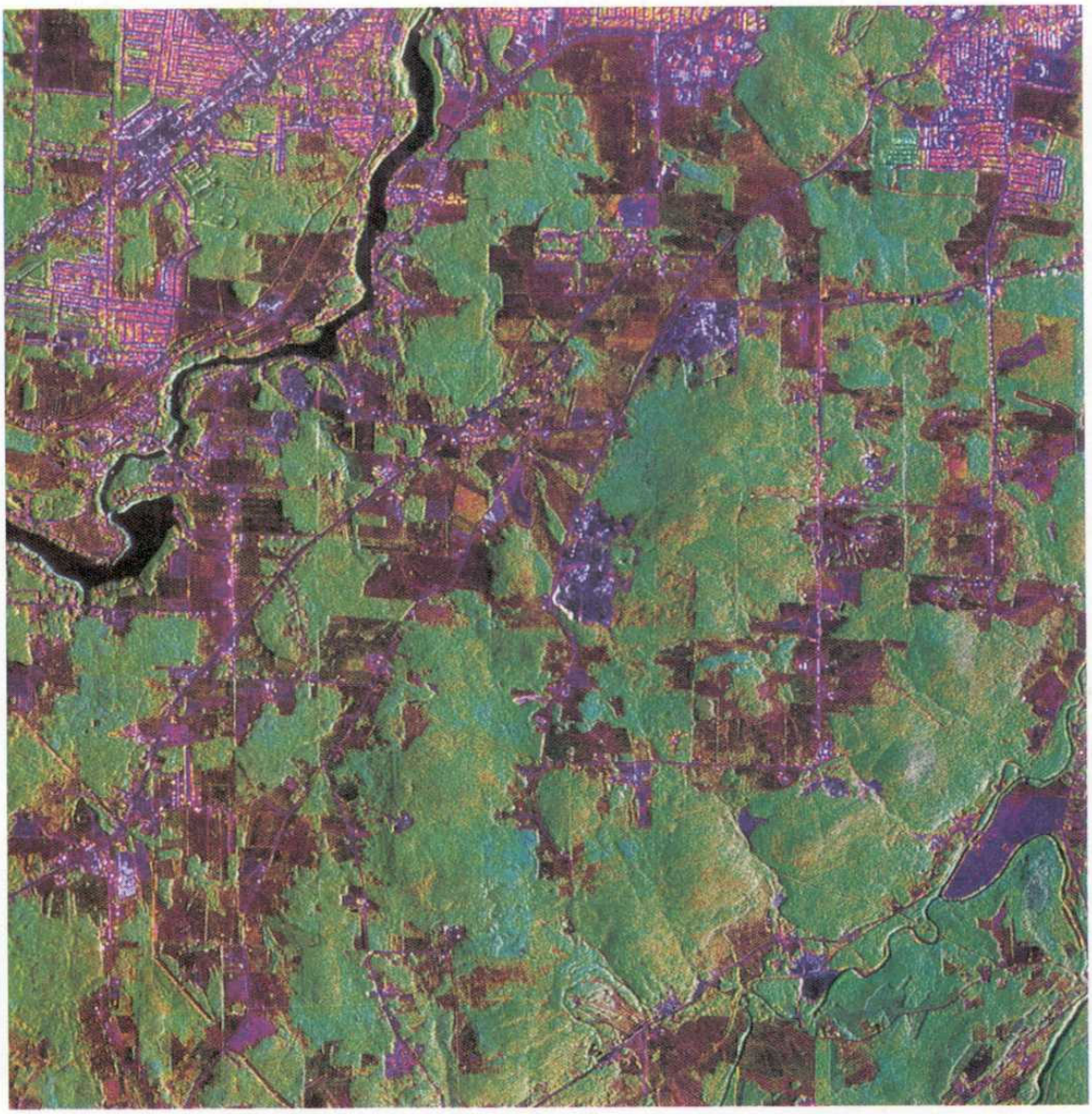

Figure 5. Sous-ortho-image composée (10 km sur 10 km; pixel de 5 m) en utilisant le codage ITS (RAS-ouest/SPOT-P/RAS-est).

Figure 5: Composite subortho-images (10 x 10 km; 5 m pixel spacing) using IHS coding (SAR-west/SPOT-P/SAR-east)

In the image in Figure 4, the white spots represent suspended sediments, although in certain places they could be reflections off a rough surface, such as at the dam. This information is less visible on the image in Figure 3 and invisible on the other image (Figure 5).

The image in Figure 4 provides no information on the topography, as the SAR characteristics, which are sensitive to relief are not visible. In the other two images (Figure 3 and 5), the shadows and their orientation are enhanced by the use of two SARs of opposite viewing directions. In Figure 5, moreover, the coding of the SAR-west mosaic in intensity accentuates the texture of the image.

4.2.2 Agriculture

The boundaries of fields are clearly visible in all three images; in Figures 3 and 5, these boundaries are enhanced by fences, which are highly visible because of the SAR information figuring prominently in these images. For the same reason, fields containing stumps or undergoing reforestation are identifiable. As the dynamic range is greater in the Figure 3 image, it allows better discrimination between land uses and between bared and cultivated fields.

4.2.3 Forestry

All three images are very good for distinguishing forest from everything else. However, it is practically impossible to distinguish between deciduous and coniferous trees, except in certain places in the image in Figure 4. This must come from the SPOT-P intensity image, since conifers are darker in SPOT-P images.

In the Figure 3 image, we can see texture on the tree canopy which is related to the size of the crown and not to tree type (deciduous versus coniferous). Rows of isolated trees are also visible because of their shadow.

In the image in Figure 5, there is a visual impression of tree height superimposed on the relief, allowing us to interpret the characteristics and disturbances of stands on the basis of forest cover height. Moreover, this impression, combined with the shading, lets us distinguish rows of isolated trees.

4.2.4 Geology

When relief is not useful, all three images allow the distinction of more or less the same geomorphologic elements: the two NE-SW rivers and their characteristics (meanders, embankments, bars). However, as soon as interpretation requires knowledge of the relief, the images in Figures 3 and 5 are more useful: stream bank slopes and glacial formations, with drumlins and ridges, which indicate the NE-SW ice advance. Similarly, NE-SW lineaments and folds, identifiable only on these two images, are probably related to the structural trend of the region.

According to these comparisons for the various applications, the combinations which have preserved the integrity of the original data have the greatest potential; these are the GRB coding and IHS coding, assigning SAR-west/SPOT-P/SAR-east respectively.

This last combination seemed to be the most logical in our case, since SPOT-P covers the visible spectrum, and the higher-resolution SAR images (4 m versus 10 m), with more texture, modulate intensity and saturation better, corresponding to the tests and results of Jaskolla et al (1988) and Welch and Ehlers (1988).

5. CONCLUSION

With the goal of evaluating quantitatively and qualitatively the impact of geometric and radiometric processing techniques on the creation of composite products which integrate images from multiple sensors (SPOT-P and SAR) and geocoded data from

other sources (digital elevation model, digital file of position data for cartographic elements), this article has compared:

- for geometric processing, polynomial methods of the 2nd and 3rd orders and the photogrammetric method;
- for radiometric processing, various codings (RGB, PC, IHS and HPF) to merge the spectral information.

5.1 Geometric processing

As predicted in theory, the photogrammetric method demonstrated its superiority and greater effectiveness compared to the polynomial methods (2nd and 3rd orders) for the two types of images.

The polynomial method of the 3rd order is no improvement over the 2nd order and even lowers the quality of the ortho-image: the contribution of the 3rd-order terms (x^3, x^2y, xy^2, y^3) to correction of the images is negligible (less than 0.10 m).

This superiority of the photogrammetric method is due mainly to the fact that the mathematical model corresponds to the physical reality of the viewing geometry and takes into account the distortions caused by relief. Since the elevation difference is not very large (350 m) in our study site, this superiority will increase with greater elevation differences.

The impact on the creation of composite ortho-images is of two kinds, quantitative and qualitative:

- relative accuracy of one pixel (5 m) and 4-5 pixels for the photogrammetric and polynomial methods respectively;
- absolute accuracy of 10 m and 30-40 m for the photogrammetric and polynomial methods respectively;
- for the photogrammetric method: a sharper and more precise image of better quality which is closer to reality, on which the cartographic elements are well defined and easier to interpret;
- for the polynomial method: a more blurred image with cartographic elements that are less contrasted and thus difficult to interpret and define; an image having less integrity, with the creation of artifacts and information not corresponding to reality.

In the first method, subsequent processing operations will be facilitated, while in the second, more complicated processing operations will be required to remove the artifacts and false information. However, because the latter do not correspond to any physical reality and depend on viewing conditions (images, ground and so on), the subsequent methods and processing techniques developed for one set of multisource images under specific conditions will apply with great difficulty or not at all to another set of multisource images under different conditions, thus limiting the use and future applications of such composite images.

5.2 Radiometric processing

Two codings were eliminated from the comparisons: the HPF, because it does not apply to this data set, and PCs, because they do not preserve the integrity of the original data due to arithmetic/statistical transformations of the radiometry.

The codings which showed the greatest potential are the colour display transformations, RGB and IHS, which do not transform the radiometry. Of these, the combinations in which the nature and characteristics of the original data are best preserved (SPOT-P/SAR-west/SAR-east in RGB and HIS respectively) were qualitatively compared for four conventional applications of remote sensing: topography, agriculture, forestry and geology. The two combinations give more or less equivalent results, with a plus for IHS in forestry and geology because of the texture and impression of relief of the trees, and a plus for RGB in agriculture due to the better dynamic range from the more visible SPOT-P.

Finally, the registration of remote sensing multisource data to vector data in geographic information systems requires rigorous geometric correction methods to obtain subpixel accuracy, as well as radiometric processing techniques which take into account the nature and characteristics of the data to ensure that the composite image preserves the best of the information from each image and maintains data integrity.

ACKNOWLEDGMENTS

The author would like to thank the following CCRS scientists for their collaboration in interpreting the composite images: Frank Ahern, Brian Brisco, Douglas O'Brien and Vernon Singhroy. He would also like to thank Réjean Simard and Philippe Teillet of CCRS for the revision and critical comments. The image processing was performed by Ms Liyuan Wu of Consultants TGIS Inc, and the computer aspects related to the SRIT software ("Système de Rectification des Images de Télédétection") were handled by François Naud of Consultants TGIS Inc.

REFERENCES

Anuta, P.E., Freeman, D.M., Shelly, B.M. and Smith, C.R., 1978, SAR-Landsat image registration systems study, LARS Contract Report 082478, Purdue University, Ind., U.S.A.

Chavez, P.S. Jr., Sides, S.C. et Anderson, J.A., 1991, Comparison of three different methods to merge multiresolution and multispectral data: Landsat-TM and SPOT panchromatic, *Photogrammetric Engineering and Remote Sensing*, 57(3), 295-303.

Clark, J., 1980, Training site statistics from Landsat and Seasat satellite imagery registered to a common map base, *Proceedings of the ASPRS Semi-Annual Convention*, held in Niagara Falls, (U.S.A., American Society of Photogrammetry), RS.1.F.1-RS.1.F.9

Colwell, R.N., 1983, *Manual of Remote Sensing*, 2nd edition, Vol. 1, (Falls Church, Virginia, U.S.A., Sheridan Press).

Daily, M., Farr, T., Elachi, C. and Schuber, G., 1979, Geologic interpretation from composite radar and Landsat imagery, *Photogrammetric Engineering and Remote Sensing*, 45(8), 1109-1116.

Guertin, F., and Shaw, E., 1981, Definition and potential of geocoded satellite imagery products, *Proceedings of the 7th Canadian Symposium on Remote Sensing*, held in Winnipeg, Canada, September 8-11, (Manitoba Remote Sensing Centre, Canada), 384-394

Guindon, B., Harris, J.W.E., Teillet, P.M., Goodenough, D.G. and Meunier, J.F., 1980, Integration of MSS and SAR data for forested regions in mountainous terrain, *Proceedings of the 14th International Symposium of Remote Sensing Engineering* held in San Jose, Costa Rica, (USA, ERIM), 79-84.

Guindon, B., 1985, Automated control point acquisition in radar optical image registration, *Canadian Journal of Remote Sensing*, 11(1), 103-112.

Harris, J.R., Murray, R. and Hirose, T., 1990, IHS transform for the integration of radar imagery with other remotely sensed data, *Photogrammetric Engineering of Remote Sensing*, 56(2), 1631-1641.

Jaskolla, F., Rast, M., and Bodechtel, J., 1985, The use of SAR system for geological applications, *Proceedings of the Workshop on Thematic Applications of SAR Data*, held in Frascati, Italy, SP-257, (Paris, ESA), 41-50.

Lasserre, M., et Lemieux, J.P., 1990, Zone d'essai de Sherbrooke pour les applications topographiques de la télédétection, Rapport final, Énergie, Mines et Ressources Canada.

Livingstone, C.E., Gray, A.L., Hawkins, R.K., Olsen, R.B., Halbertsma, J.G., et Deane, R.A., 1987, CCRS C-band airborne radar: system description and test results, *Proceedings of the 11th Canadian Symposium on Remote Sensing*, held in Waterloo, Canada, 22-25 June, (University of Waterloo, Canada), 379-395.

Murphrey, S.W., 1978, SAR-Landsat image registration study, Final report, IBM Corp., Gaithersburg, MD, U.S.A.

Toutin, Th., 1986, Étude mathématique pour la rectification d'images SPOT, *Compte-rendus du XVIIIe Congrès international des géomètres*, tenu à Toronto, Canada, 1-11 juin, (Institut canadien des levés, Ottawa, Canada), 379-395.

Toutin, Th., et Carbonneau, Y., 1989, La multi-stéréoscopie pour les corrections d'images SPOT-HRV, *Journal canadien de télédétection*, 15(2), 110-119.

Toutin, Th., et Carbonneau, Y., 1992, La création d'ortho-images avec MNA : description d'un nouveau système, *Journal canadien de télédétection*, 18(3), 136-141.

Toutin, Th., Carbonneau, Y., et St-Laurent, L., 1992, An integrated method to rectify airborne radar imagery using DEM, *Photogrammetric Engineering and Remote Sensing*, 58(4), 417-422.

Welch, R. and Ehlers, M., 1988, Cartographic feature extraction with integrated SIR-B and Landsat-TM images, *International Journal of Remote Sensing*, 9(5), 873-889.

Zobrist, A.L., Blackwell, R.J., and Stromberg, W.D., 1979, Integration of Landsat, Seasat and other geodata sources, *Proceedings of the 13th Annual Symposium on Remote Sensing of the Environment*, held in Ann Arbor, (U.S.A., ERIM), 271-279.